Image Variational Decomposition Based on Dual Method

Ruihua Liu[1,2] and Ruizhi Jia[1]

[1]*School of Mathematics and Statistics,*
Chongqing University of Technology, Chongqing, China, 400050
[2]*Institute of Automation, Chinese Academy of Sciences, Beijing, China, 100090*
lruih@sohu.com

Abstract

In the paper, we firstly recommend a new variational model for image decomposition into cartoon and texture or noise by introducing a new function in Sobolev space, in order to overcome the inconsistency between the theoretical model and numerical simulation. Secondly, we prove the existence of minimal solutions of the improved ROF energy functional. Subsequently, we also introduce two additional improved models in the same way. Finally, we show some numerical experiments of our improved ROF models, and correspondingly compare them with those of the ROF model, VO model and TV-$\mathcal{H}^{-1}$ model. The results show that our models work well.

Keywords: *Image decomposition, variational approach, minimal solution, cartoon, texture*

1. Introduction

Decomposing an image into meaningful components is an important and challenging inverse problem in image processing. Let f be an observed image which contains texture and/or noise. Texture is characterized as repeated and meaningful structure of small patterns. We are interested in decomposing f into two components $f = u + v$, such that u represents cartoon part of f, which is the geometric or structural component of f, while v is the oscillating or texture component of f. PDE-based methods have been widely used over the past decade for image decomposing [1-15].

In 1992, Rudin et al.[13] proposed a TV-L^2 model (ROF) used to remove the noise. This algorithm can be used to image decomposition. The model is defined as a variational problem

$$\min_u E(u) = \int_\Omega |Du| + \lambda \|v\|^2_{L^2(\Omega)}. \tag{1.1}$$

Where $\lambda > 0$, $u \in \mathrm{BV}(\Omega)$ represents cartoon part, $v = f - u$ is texture part. In 2011, Meyer[10] pointed out some limitations of the ROF model and proposed a different decomposition model which was called the TV-G model. The model is described as the following form

$$\min_u E(u) = \int_\Omega |Du| + \lambda \|v\|_G, \tag{1.2}$$

where $v = f - u$, $u \in \mathrm{BV}(\Omega)$, λ>0. The Banach space G contains signals with large oscillations, such as texture or noise. It is well known that the G-norm captures oscillatory patterns and texture better than the standard ROF model does, but the TV-G model is difficult to implement due to the nature of the G-norm. In 2003, Vese el at.[14] proposed firstly a

numerical scheme to solve this model using Euler-Lagrange equations based on L^p -norms. Then they proposed the G- norm in the following energy

$$\min_{u,g_1,g_2} E(u,g_1,g_2)=\int_\Omega |Du|+\mu\|\nabla g\|_{L^p(\Omega)}+\frac{\lambda}{2}\|f-u-\partial_x g_1-\partial_y g_2\|^2_{L^2(\Omega)}, \qquad (1.3)$$

where $g=(g_1,g_2)$, $div\ g\approx v=f-u\in G$, λ, $\mu>0$, $u\in \mathrm{BV}(\Omega)$. The model is also called VO model. Subsequently, Aujol et al. [2-3,10,15] provided some numerical schemes to compute the TV-G model. In 2003, Osher et al.[12] offered a new image decomposition model using the $\mathcal{H}^{-1}$ -norm. The functional to minimize in this case is

$$\min_{\Omega} E(u)=\int_\Omega |Du|+\frac{\lambda}{2}\|\nabla\Delta^{-1}v\|^2_{L^2(\Omega)}, \qquad (1.4)$$

where $v=f-u$, $u\in \mathrm{BV}(\Omega)$, $\lambda>0$. The authors showed that the TV-$\mathcal{H}^{-1}$ model was simpler than the VO model did, because of the fewer parameters tuned and just one unknown function solved in the TV-$\mathcal{H}^{-1}$ model. In 2004, Nikolova[11] proved a TV-L^1 model because L^1-norm was particularly well suited to remove salt and pepper noise. The model can better protect structures and present other interesting properties than the ROF model does. In 2008, Lieu el at.[9] proposed a class of TV-$\mathcal{H}^{-s}$ models for image decomposition following the idea of the Meyer's idea.

The cartoon component u of f belongs to BV space in the all of above models. It is well known that the functional norm of BV space function is defined as follows

$$\int_\Omega |Du|=\sup\left\{\int u\,div\varphi \,\middle|\, \varphi=(\varphi_1,\varphi_2,\cdots,\varphi_n)\in C_0^1(\Omega)^N\right\}, \qquad (1.5)$$

where $\|\varphi\|_{L^\infty(\Omega)}\le 1$. But it is difficult to find such a function φ when we take the numerical implementation. So we generally transfer the regularization term $\int_\Omega |Du|$ into the $\|\nabla u\|_{L^1(\Omega)}$ term, that is, u belongs to the Sobolev space, which will cause the inconsistency between the theoretical model and numerical simulation. Happily, Bresson el at.[6] introduced a new function w in $\mathrm{W}^{1,1}$ space to close in the function u in BV space in their active contour model in order to overcome the above mentioned defect. They relax the energy functional of the TV regularization term $\|u\|_{BV(\Omega)}$ as

$$\min_{u,w} E(u,w)=\|\nabla w\|_{L^1(\Omega)}+\lambda\|u-w\|^2_{L^2(\Omega)}. \qquad (1.6)$$

In this work, we develop a global minimization model for image decomposition inspired by [6]. Besides, we give its theoretical proof of existence of solution of the minimal functional, and also propose a numerical scheme to perform the evolution equations in an efficient. Finally, we also recommend another two models by the same approach.

The rest of the paper is organized as follows. In Section 2, we formulate a novel image decomposition model inspired by [6], and provide the evolvement equations. In Section 3, we main theoretically prove the existence of minimizer of our proposed model. In Section 4, we deal with additional models by the same method. In Section 5, we show the numerical experimental results, and compare the results of our proposed model with those of the ROF model, VO model and TV-$\mathcal{H}^{-1}$ model, respectively. In Section 6, we give some conclusions and discussions.

2. Our Proposed Mathematical Model

In this section, we introduce our model which is inspired by the work [6]. We first present it in the continuous setting. Then we provide a mathematical study for the model.

Considering an image f which contains cartoon and texture, can be decomposed into two components $u+v$. The first component u is so-called cartoon part, and has a simple geometric description. The second component v contains texture or noise.

According to the above analysis in section 1, then we propose the following minimization problem, inspired by the work [6] and ROF model

$$\min_{u,w} E(u,w) = \|\nabla w\|_{L^1} + \frac{1}{2\theta}\|w-u\|_{L^2}^2 + \frac{\lambda}{2}\|f-u\|_{L^2}^2, \tag{2.1}$$

where $v = f-u$, $w \in \mathrm{W}^{1,1}(\Omega)$, $u \in L^2(\Omega)$, λ and θ are positive parameters. The model is called as the improved ROF model.

The energy functional (2.1) may be minimized using a multitude of optimization procedures. In order to avoid the scale problem and for algorithm simplicity, we propose the following alternating iterative minimization procedure. Let us denote

(i) $\min_{w} E(u,w|u) = E(u,w)$ with u fixed;

(ii) $\min_{u} E(u,w|w) = E(u,w)$ with w fixed.

Then, we follow the idea of coordinate descent to minimize by alternating the minimization of (i) and (ii) iteratively. The global convergence of the algorithm to one of the local minima of the functional $E(u,w)$ can be established by noting the fact[8]. Here, we use the idea of the steepest descent to find the solution to those minimization problems in (i) and (ii). Let us write down the evolvement equations

$$\frac{\partial w}{\partial \tau_0} = div\left(\frac{\nabla w}{|\nabla w|}\right) - \frac{1}{\theta}(w-u), \tag{2.2}$$

$$\frac{\partial u}{\partial \tau_1} = \frac{1}{\theta}(w-u) + \lambda(f-u). \tag{2.3}$$

3. Existence of Minimal Solutions

In this section, we prove existence of minimizer for the improved ROF model, adapting the technique in the work [1]. For simplifying the theoretical proof, we introduce a function w in BV space of the functional, and relax the functional into the following form:

$$\min_{w,u} E^{\varepsilon}(w,u) = \|\nabla w\|_{L^1} + \frac{1}{2\theta}\|w-u\|_{L^2}^2 + \frac{\lambda}{2}\|f-u\|_{L^2}^2 + \frac{\varepsilon}{2}\int_{\Omega}\left(w^2 + |\nabla w|^2\right). \tag{3.1}$$

where $v = f-u$, $u \in L^2(\Omega)$, $w \in \mathrm{W}^{1,2}(\Omega)$, λ>0.

Proposition 3.1 Fix $\varepsilon > 0$, then there is a minimal solution $\left(\hat{w}^{\varepsilon}, \hat{u}^{\varepsilon}\right) \in \mathrm{W}^{1,2}(\Omega) \times L^2(\Omega)$ of the problem (3.1).

Proof: Fix $\varepsilon > 0$, it is clear that $E^{\varepsilon}(u, w)$ is coercive. Suppose $\left(w_n^{\varepsilon}, u_n^{\varepsilon}\right) \in \mathrm{W}^{1,2}(\Omega) \times L^2(\Omega)$ is a minimizing sequence for the problem (3.1), then we can obtain

$$\left\|\nabla w_n^{\varepsilon}\right\|_{L^2} \le \mathrm{M}, \ \left\|w_n^{\varepsilon}\right\|_{L^2} \le \mathrm{M}, \ \left\|u_n^{\varepsilon}\right\|_{L^2} \le \mathrm{M}. \tag{3.2}$$

Therefore, we get that w_n^{ε} and u_n^{ε} are bounded in $\mathrm{W}^{1,2}(\Omega)$ and $L^2(\Omega)$, respectively. Then there exist $\hat{w}^{\varepsilon}$ and $\hat{u}^{\varepsilon}$ in $\mathrm{W}^{1,2}(\Omega)$ and $L^2(\Omega)$, and two subsequences such that $w_n^{\varepsilon} \to \hat{w}^{\varepsilon}$ in $\mathrm{W}^{1,2}$-weak and $u_n^{\varepsilon} \to \hat{u}^{\varepsilon}$ in L^2-weak. According to the convexity, we gain that $\left(\hat{w}^{\varepsilon}, \hat{u}^{\varepsilon}\right)$ is a solution of problem (3.1).

Proposition 3.2 Fix $\varepsilon > 0$, if $\left(\hat{w}^{\varepsilon}, \hat{u}^{\varepsilon}\right)$ is a solution of problem (3.1), then they separately satisfy the Euler-Lagrange equations

$$-div\left(\frac{\nabla \hat{w}^{\varepsilon}}{\left|\nabla \hat{w}^{\varepsilon}\right|}\right) + \frac{1}{\theta}\left(\hat{w}^{\varepsilon} - \hat{u}^{\varepsilon}\right) + \varepsilon \hat{w}^{\varepsilon} - \varepsilon \Delta \hat{w}^{\varepsilon} = 0, \tag{3.3}$$

$$-\frac{1}{\theta}(\hat{w}^{\varepsilon} - \hat{u}^{\varepsilon}) - \lambda(f - \hat{u}^{\varepsilon}) = 0. \tag{3.4}$$

with the Neumann boundary condition, $\frac{\partial \hat{w}}{\partial \vec{N}} = 0$.

Proposition 3.3 Fix $\varepsilon > 0$, suppose $f \in L^{\infty}(\Omega)$, and $\left(\hat{w}^{\varepsilon}, \hat{u}^{\varepsilon}\right)$ be a solution of problem (3.1). Then, we have $ess\inf_{\Omega} f \le \hat{w}^{\varepsilon} \le ess\sup_{\Omega} f$, $ess\inf_{\Omega} f \le \hat{u}^{\varepsilon} \le ess\sup_{\Omega} f$.

Proof: Let $k = ess\sup_{\Omega} f$, $G \in C^1$ is a truncation function, $G(t) = 0$ on $[0, +\infty)$ and $G(t)$ is strictly increasing on $(0, +\infty)$. Given $v = G(\hat{w}^{\varepsilon} - k)$, and then $\nabla v = G'(\hat{w}^{\varepsilon} - k) \cdot \nabla \hat{w}^{\varepsilon}$. We multiply equation (3.3) by v and integrate in Ω, hence we get

$$\int_{\Omega} \left|\nabla \hat{w}^{\varepsilon}\right| \cdot G'\left(\hat{w}^{\varepsilon} - k\right) dx + \frac{1}{\theta} \int_{\Omega} \left(\hat{w}^{\varepsilon} - \hat{u}^{\varepsilon}\right) \cdot G\left(\hat{w}^{\varepsilon} - k\right) dx$$

$$+ \varepsilon \int_{\Omega} \hat{w}^{\varepsilon} \cdot G\left(\hat{w}^{\varepsilon} - k\right) dx + \varepsilon \int_{\Omega} \left|\nabla \hat{w}^{\varepsilon}\right|^2 \cdot G'\left(\hat{w}^{\varepsilon} - k\right) dx = 0. \tag{3.5}$$

Since $G' \ge 0$ and $G \ge 0$, we can obtain

$$\frac{1}{\theta} \int_{\Omega} \left(\hat{w}^{\varepsilon} - \hat{u}^{\varepsilon}\right) \cdot G\left(\hat{w}^{\varepsilon} - k\right) dx + \varepsilon \int_{\Omega} \hat{w}^{\varepsilon} \cdot G\left(\hat{w}^{\varepsilon} - k\right) dx \le 0. \tag{3.6}$$

i.e.,

$$\int_{\left(\frac{1}{\theta}+\varepsilon\right)\hat{w}^{\varepsilon}>\frac{1}{\theta}\hat{u}^{\varepsilon}}\left(\left(\frac{1}{\theta}+\varepsilon\right)\hat{w}^{\varepsilon}-\frac{1}{\theta}\hat{u}^{\varepsilon}\right)\cdot G\left(\hat{w}^{\varepsilon}-k\right)+\int_{\left(\frac{1}{\theta}+\varepsilon\right)\hat{w}^{\varepsilon}\le\frac{1}{\theta}\hat{u}^{\varepsilon}}\left(\left(\frac{1}{\theta}+\varepsilon\right)\hat{w}^{\varepsilon}-\frac{1}{\theta}\hat{u}^{\varepsilon}\right)\cdot G\left(\hat{w}^{\varepsilon}-k\right)\le 0. \tag{3.7}$$

Thus, $\int_{\left(\frac{1}{\theta}+\varepsilon\right)\hat{w}^{\varepsilon}>\frac{1}{\theta}\hat{u}^{\varepsilon}}\left(\left(\frac{1}{\theta}+\varepsilon\right)\hat{w}^{\varepsilon}-\frac{1}{\theta}\hat{u}^{\varepsilon}\right)\cdot G\left(\hat{w}^{\varepsilon}-k\right)\le 0.$ In fact, it is equal to zero since $G\ge 0$.

Therefore, $\left|\Omega_{\left(\left(\frac{1}{\theta}+\varepsilon\right)\hat{w}^{\varepsilon}>\frac{1}{\theta}\hat{u}^{\varepsilon}\right)}\right|=0,$ where $|\cdot|$ is Lévesque measure, then, $\left(\frac{1}{\theta}+\varepsilon\right)\hat{w}^{\varepsilon}\le\frac{1}{\theta}\hat{u}^{\varepsilon}$.

According to (3.4), we have $\hat{u}^{\varepsilon}=\frac{\hat{w}^{\varepsilon}+\theta\lambda f}{1+\theta\lambda}$. Furthermore, we derive

$$\hat{u}^{\varepsilon}\le\frac{\lambda+\lambda\theta\varepsilon}{\lambda+\varepsilon+\lambda\theta\varepsilon}f\le ess\sup_{\Omega} f=k,\ \hat{w}^{\varepsilon}\le\hat{u}^{\varepsilon}\le k. \tag{3.8}$$

Similarly, we can get $ess\inf_{\Omega} f\le\hat{u}^{\varepsilon}$, $ess\inf_{\Omega} f\le\hat{w}^{\varepsilon}$.

Theorem Let $f\in L^{\infty}(\Omega)$, then there is at least one minimal solutions of the minimization functional (2.1).

Proof: Based on the above discussions, we have

$$E^{\varepsilon}\left(\hat{w}^{\varepsilon},\hat{u}^{\varepsilon}\right)\le E^{\varepsilon}\left(w,u\right),\forall w\in \mathrm{W}^{1,2},\ u\in L^{2}. \tag{3.9}$$

Especially, we take $w=1,\ u=1$, then

$$\left\|\nabla\hat{w}^{\varepsilon}\right\|_{L^1}\le \mathrm{M},\ \left\|\hat{w}^{\varepsilon}\right\|_{L^1}\le \mathrm{M},\ \left\|\hat{u}^{\varepsilon}\right\|_{L^2}\le \mathrm{M}. \tag{3.10}$$

We can obtain that $\hat{w}^{\varepsilon}$ is uniformly bounded in $\mathrm{W}^{1,1}$ space and BV space. Thus there exists a subsequence and $\hat{w}$ in BV space such that $\hat{w}^{\varepsilon}\to\hat{w}$ in $\mathrm{BV}-w^{*}$ and $\hat{w}^{\varepsilon_n}\to\hat{w}$ in L^1-strong. At the same time, $\hat{u}^{\varepsilon}$ is uniformly bounded in L^2 space, then there is a subsequence and $\hat{u}$ in L^2 space such that $\hat{u}^{\varepsilon}\to\hat{u}$ in L^2-weak. According to the convexity, we obtain

$$\begin{aligned}&E\left(\hat{w},\hat{u}\right)\le\liminf_{\varepsilon\to 0}E^{\varepsilon}\left(\hat{w}^{\varepsilon},\hat{u}^{\varepsilon}\right)\\&=\liminf_{\varepsilon\to 0}\left\{\int_{\Omega}\left|\nabla\hat{w}^{\varepsilon}\right|+\frac{1}{2\theta}\left\|\hat{w}^{\varepsilon}-\hat{u}^{\varepsilon}\right\|_{L^2}^{2}+\frac{\lambda}{2}\left\|f-\hat{u}^{\varepsilon}\right\|_{L^2}^{2}+\frac{\varepsilon}{2}\int_{\Omega}\left(\left(\hat{w}^{\varepsilon}\right)^{2}+\left|\nabla\hat{w}^{\varepsilon}\right|^{2}\right)\right\}.\end{aligned} \tag{3.11}$$

So, $\left(\hat{w},\hat{u}\right)\in \mathrm{BV}(\Omega)\times L^{2}(\Omega)$ is a minimal solution of the minimization functional (2.1).

4. Additional Improved Models

In this section, we introduce additional two improved models by the same approach. One is the improved VO model, the other is the improved TV-$\mathcal{H}^{-1}$ model. The improved VO model will be the following form

$$\min_{w,u,g_1,g_2} E(w,u,g_1,g_2) = \|\nabla w\|_{L^1} + \frac{1}{2\theta}\|w-u\|_{L^2}^2 + \mu\|\nabla g\|_{L^p} + \frac{\lambda}{2}\|f-u-\partial_x g_1-\partial_y g_2\|_{L^2}^2 \quad , \qquad (4.1)$$

where λ, μ and θ are positive parameters $g=(g_1,g_2)$, $div\, g \approx v = f-u \in G$, $w \in \mathrm{W}^{1,1}$, $u \in L^2$, Thus, the corresponding evolution equations are the form

$$\frac{\partial w}{\partial \tau_0} = div\left(\frac{\nabla w}{|\nabla w|}\right) - \frac{1}{\theta}(w-u), \qquad (4.2)$$

$$\frac{\partial u}{\partial \tau_1} = \frac{1}{\theta}(w-u) + \lambda(f-u-\partial_x g_1-\partial_y g_2), \qquad (4.3)$$

$$\frac{\partial g_1}{\partial \tau_3} = \lambda\left[(u-f)_x + \partial_{xx} g_1 + \partial_{xy} g_2\right] - \mu\left(\left\|\sqrt{g_1^2+g_2^2}\right\|_p\right)^{1-p}\left(\sqrt{g_1^2+g_2^2}\right)^{p-2} g_1, \qquad (4.4)$$

$$\frac{\partial g_2}{\partial \tau_4} = \lambda\left[(u-f)_y + \partial_{xy} g_1 + \partial_{yy} g_2\right] - \mu\left(\left\|\sqrt{g_1^2+g_2^2}\right\|_p\right)^{1-p}\left(\sqrt{g_1^2+g_2^2}\right)^{p-2} g_2. \qquad (4.5)$$

Similarly, we propose the improved TV-$\mathcal{H}^{-1}$ model

$$\min_{w,u} E(w,u) = \|\nabla w\|_{L^1} + \frac{1}{2\theta}\|w-u\|_{L^2}^2 + \frac{\lambda}{2}\|\nabla\Delta^{-1}(f-u)\|_{L^2}^2. \qquad (4.6)$$

where $v=f-u$, $w \in \mathrm{W}^{1,1}$, $u \in L^2$, λ and θ are positive parameters. In the same way, we come up with the evolvement equations

$$\frac{\partial w}{\partial \tau_0} = div\left(\frac{\nabla w}{|\nabla w|}\right) - \frac{1}{\theta}(w-u), \qquad (4.7)$$

$$\frac{\partial u}{\partial \tau_1} = -\frac{1}{\theta}\Delta(w-u) + \lambda(f-u). \qquad (4.8)$$

5. Numerical Experiments

In this section, we show some numerical results using our three provided models, and compare them with those of by ROF model [13], TV-$\mathcal{H}^{-1}$ model [12] and VO model [14].

In the following experiments, we use three standard high-resolution images as experiments, such as Logo image, Lena image and Barbara image.

(a) (b) (c)

Figure 1. Test Original Images: (a) Lena Image, (b) Logo Image, (c) Barbara Image

(a) (b) (c) (d)

Figure 2. Lena Image Decomposition and Comparison: (a) Cartoon Part by ROF Model, (b) Texture Part by ROF Model, (c) Cartoon Part by Our Improved ROF Model, (d) Texture Part by Our Improved ROF Model

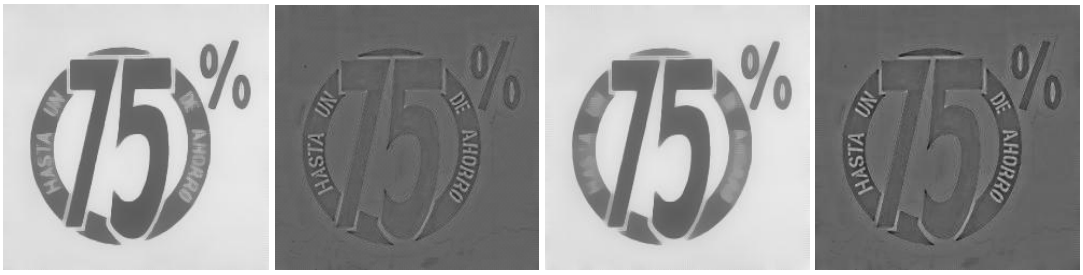

(a) (b) (c) (d)

Figure 3. Logo Image Decomposition and Comparison: (a) Cartoon Part by ROF Model, (b) Texture Part by ROF Model, (c) Cartoon Part by Our Improved ROF Model, (d) Texture Part by Our Improved ROF Model

Figure 2 and Figure 3 demonstrate two simulation results by decomposing Lena image and Logo image. Through comparing the cartoon parts of Figure 2(a) and Figure 3(a) by ROF model with those of Figure 2(c) and Figure 3(c) by our improved ROF model, respectively, besides the texture parts of Figure 2(b) and Figure 3(b) by ROF model with those of Figure 2(d) and Figure 3(d), respectively, we can see that the cartoon parts in Figure 2(a) and Figure 3(a) involve more texture than those in Figure 2(c) and Figure 3(c), but the parts in Figure 2(b) and Figure 3(b) include less texture than those in Figure 2(d) and Figure 3(d). So, we can get that the decomposition effects by our improved ROF model achieve better than those by ROF model does.

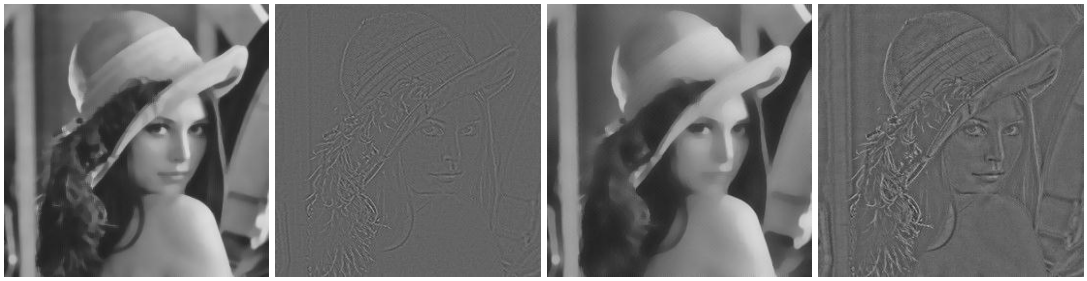

(a) (b) (c) (d)

Figure 4. Lena Image Decomposition and Comparison: (a) Cartoon Part by TV-$\mathcal{H}^{-1}$ Model, (b) Texture Part by TV- $\mathcal{H}^{-1}$ Model, (c) Cartoon Part by Our Improved TV-$\mathcal{H}^{-1}$ Model, (d) Texture Part by Our Improved TV-$\mathcal{H}^{-1}$ Model

Figure 4 shows one experimental result by decomposing Lena image. After comparing the cartoon part of Figure 4(a) by TV-$\mathcal{H}^{-1}$ model with that of Figure 4(c) by our improved TV-$\mathcal{H}^{-1}$ model, and the texture part of Figure 4(b) by TV-$\mathcal{H}^{-1}$ model with that of Figure 4(d), respectively, we find that the part in Figure 4(a) involve more texture than that in Figure 4(c), but the part in Figure 4(b) include less texture than that in Figure 4(d). Then, we can derive that the effect by our improved TV-$\mathcal{H}^{-1}$ model infers better than that by TV-$\mathcal{H}^{-1}$ model does. In addition, we also detect that the TV-$\mathcal{H}^{-1}$ model is excel to the ROF model by contracting Figure 2(b) to Figure 4(b), and our improved TV-$\mathcal{H}^{-1}$ model can more fit to image decomposition by comparing Figure 2(c) with Figure 4(c) because of the excessive stair-case effect in Figure 2(c).

(a) (b) (c) (d)

Figure 5. Barbara Image Decomposition and Comparison. (a) Cartoon Part by VO Model, (b) Texture Part by VO Model, (c) Cartoon Part by Our Improved VO Model, (d) Texture Part by Our Improved VO Model

Figure 5 shows one experiment by decomposing Barbara image. By comparing the cartoon part of Figure 5(a) by VO model with that of Figure 5(c) by our improved VO model, and the texture part of Figure 5(b) by VO model with that of Figure 5(d), respectively, we can see that the effect of VO model is close on that of our improved VO model.

6. Conclusions and Discussions

By the above theory analysis and numerical simulations, we can see that our three proposed models are very effect for image decomposition. The alternating iterative minimization algorithm is also feasible. If we only consider the experimental results, we are willing to recommend our improved TV-$\mathcal{H}^{-1}$ model.

In the paper, we only prove the existence of minimal solutions of the improved ROF model energy functional, but don't prove the existence and uniqueness of minimal solutions of the evolution equations and the existence of minimal solutions of the other two models. We will do our best to settle these problems in the future.

Acknowledgements

The work is supported by National Science Foundation of China(10971239), Natural Science Foundation Project of CQ CSTC(CSTC2011JJA40033).

References

[1] G. Aubert and J. Aujol, "A variational approach to remove multiplicative noise", SIAM J. Appl. Math., vol. 68, no. 4, **(2008)**, pp. 925-946.
[2] J. Aujol, G. Aubert, L. Blanc and A. Chambolle, "Decomposing an image: application to SAR images", Lecture Notes in Computer Science, vol. 2695, **(2003)**.
[3] J. Aujol, G. Aubert, L. Blanc and A. Chambolle, "Image decomposition into abounded variation component and an oscillating component", JMIV, vol. 22, no. 1, **(2005)**, pp. 71-88.
[4] J. Aujol and A. Chambovlle, "Dual norms and image decomposition models", International Journal of Computer Vision, vol. 63, no. 1, **(2005)**, pp. 85-104.
[5] J. Aujol, G. Gilboa, T. Chan and S. Osher, "Structure texture image decomposition modeling, algorithms and parameter selection", International Journal of Computer Imaging and Vision, vol. 20, no. 1, **(2004)**, pp. 89-97.
[6] X. Bresson, S. Esedoglu, P. Vandergheynst, J. Thiran and S. Osher, "Fast global minimization of the active contour/snake model", J. Math. Imag. Vis., vol. 28, no. 2, **(2007)**, pp. 151-167.
[7] T. Chan, S. Esedoglu and F. Park, "Image decomposition combining staircase reduction and texture extraction", UCLA CAM Report 05-18, **(2005)**.
[8] R. Lagendijk, J. Biemond and D. Boekee, "Regularized iterative image restoration with ringing reduction", IEEE Trans. on ASSP, vol. 36, no. 12, **(1988)**, pp. 1874-1887.
[9] L. Lieu and L. Vese, "Image restoration and decomposition via bounded total variation and negative Hilbert-Sobolev spaces", Appl. Math. & Opt, vol. 58, no. 2, **(2005)**, pp. 167-193.
[10] Y. Meyer, "Oscillating patterns in image processing and in some nonlinear evolution equations", The Fifteenth D. Lewis Memorial Lectures, **(2001)**.
[11] M. Nikolova, "A variational approach to remove outliers and impulse noise", JMIV, vol. 20, no. 1-2, **(2004)**, pp. 99-120.
[12] S. Osher, A. Sole and L. Vese, "Image decomposition and restoration using total variation minimization and the H^(-1) norm multiscale modeling and simulation", SIAM Interdisciplinary J., vol. 1, no. 3, **(2003)**, pp. 349-370.
[13] L. Rudin, S. Osher and E. Fatemi, "Nonlinear total variation based noise removal algorithms", Physica D, vol. 60, **(1992)**, pp. 259-268.
[14] L. Vese and S. Osher, "Modeling textures with total variation minimization and oscillating patterns in image processing", Journal of Scientic Computing, vol. 19, **(2003)**, pp. 553-572.
[15] L. Vese and S. Osher, "Image denoising and decomposition with total variation minimization and oscillatory functions", JMIV, vol. 20, no. 1, **(2004)**, pp. 7-18.

Authors

Ruihua Liu received his BSc degree in Mathematics from the Beijing Jiaotong University in 1999, his MSc degree in Mathematics from the South West China Normal University in 2005, and his PhD degree in Mathematics from the East China Normal University in 2008. He was a teacher in Wuhan University of Science & Technology from 1999 to 2002, and worked in Chongqing University of Technology from 2008. Currently, He is Post Ph.D in Institute of Automation, Chinese Academy of Sciences, and works in Beijing ViSystem Co. LTD. His research interests are image processing based on PDEs methods, and 3DMM reconstruction problems.

Ruizhi Jia received her MSc degree in Chongqing University of Technology in 2012.